Supporting materials (SM) on

The influence of nanoscale size on adsorption-desorption of U(VI) on nano-Al oxides

Tian Wan[a], Wen Cheng[a], Jiehui Ren[a], Wei Wu [a], Min Wang[a], Baowei Hu[b*], Ziyi Jia[c], Yubing Sun[d*]

[a] State Key Laboratory of Eco-Hydraulics in Northwest Arid Region, Xi'an University of Technology, Shanxi 710048, P.R. China

[b] School of Life Science, Shaoxing University, Huancheng West Road 508, Shaoxing 312000, P.R. China

[c] College of Computing, Georgia Institute of Technology, Atlanta, Georgia, USA

[d] School of environmental and chemical engineering, Xi’an Polytechnic University, P.R. China

[e] College of Environmental Science and Engineering, North China Electric Power University, Beijing, P.R. China

*Email: hbw@usx.edu.cn (B. Hu); sunyb@ncepu.edu.cn (Y. Sun)

Characterization

The protocol of acid-base titration was followed as: 0.1 g of NA or NC was added into 50 ml $NaNO_3$ solution with different concentrations (0.1, 0.01 and 0 mol/L) under vigorous stirring and N_2 conditions. The pH of suspension was adjusted to 10 with 0.05 mol/L NaOH solution, at which all deprotonated sites were $\equiv SO^-$ species, then the suspension was titrated to pH 3.5 with using 0.05 mol/L HCl solution, where all protonated sites are $\equiv SOH_2^+$. Then suspension was titrated back to pH 10 by 0.05 mol/L NaOH solution. The acid-base titration for solid free blanks was also titrated under the same protocol. The concentrations of surface reaction sites ([SOH], μmol/g) are calculated by Eqn. (S1) [1]:

$$[SOH]=0.5\times[C_{H^{+}solid+ water} - C_{H^{+}water}] \qquad (S1)$$

The protonation and deprotonation parameters (i.e., pK1 and pK2) can be calculated as Eqns. (S2)-(S3):

$$SOH_2^+ = SOH + H^+ \; pK_1 =- log\frac{[SOH]\times[H^+]}{[SOH_2^+]} =- log\frac{[SOH_{total} - Q]\times[H^+]}{Q} \quad \text{when } pH<pH_{PZC} \qquad (S2)$$

$$SOH = SO^- + H^+ \; pK_2 =- log\frac{[SO^-]\times[H^+]}{[SOH]} =- log\frac{Q\times[[H^+]}{SOH_{total} - Q} \quad \text{when } pH > pH_{PZC} \qquad (S3)$$

$$[SOH_{total}] = [SO^-] + [SOH] + [SOH_2^+] \qquad (S4)$$

$$C_B + [H^+] + [SOH_2^+] = C_A + [OH^-] + [SO^-] \qquad (S5)$$

$$C_A-C_B = [H^+] - K_w/[H^+] - [SOH_{total}](1- K_1K_2[H^+]^2/(1+ K_2[H^+] + K_1K_2[H^+]^2) \qquad (S6)$$

$$Q=(C_a-C_b+[OH^-]-[H^+])/A \qquad (S7)$$

where Kw is the water dissociation constant, $10^{-13.68}$). C_A (= C_{A0} V/(V_0+V)) and C_B (= C_{B0} V/(V_0+V)) are the actual concentration of acid and base at each point of the titration curve, respectively. Q is surface charge.

The XRD patterns were mounted with a RAPID II X-ray diffractometer equipped with autodivergent slit and graphite monochromator with a step speed of 0.02° s^{-1} at 50 kV and 50 mA. Diffractograms were obtained from 5 to 45° with a step scan increment of 0.2° and a dwell time of 2 s. The pattern was processed using JADE XRD pattern-processing software. Identification of minerals was based on comparison of the measured XRD patterns to those of mineral powder diffraction files published by the Joint Committee on Powder Diffraction Standards International Center for Diffraction Data [2].

The pore size distribution and specific surface areas were determined by nitrogen adsorption-desorption isothems at the boiling point of liquid nitrogen(77K) under atmospheric pressure using the Quantachrome NOVA 4200e instruments, with which the SSA was measured by both the multipoint BET and langmuir methods. The samples were degassed at 353 K for at least 16 h prior to the measurements. The experimentally measured saturation vapor pressure for gas-solid equilibrium at was used to assess the relative pressure in Nitrogen adsorption measurements.

For FE-TEM analysis with a Philips CM 200UT transmission electron microscope (spherical aberration coefficient=0.5mm; point-to-point resolution=0.19nm) equipped with Noran Voyager X-ray energy-dispersive spectroscopy at the Materials Science Center of the UW-Madison). The sample were mixed with methanol in an ultrasonic apparatus and superimposed on an appropriate grid of 3mm in diameter for the observation process, a drop of sample solution was applied to a carbon-coated copper grid (mesh size, 200 μm) and dried at room temperature.

Desorption kinetics

The data of adsorption kinetics were fitted by pseudo-first- order and pseudo-second-order kinetic models. The pseudo-first-order and pseudo- second-order kinetic models can be described by Eqns. S8 [3] and S9 [4], respectively:

$$\ln\left(q_e - q_t\right) = lnq_e - k_f \times t \qquad \text{(S8)}$$

$$\frac{t}{q_t} = \frac{1}{k_s \times q_e^2} + \frac{t}{q_e} \qquad \text{(S9)}$$

where q_e and q_t (mg/g) are the amount of radionuclides adsorbed at equilibrium and at time t, respectively. k_f and k_s are the pseudo-first order and pseudo-second order kinetic rate constant, respectively. The fitted results and the corresponding kinetic parameters are shown in Figure S1 and Table S1, respectively.

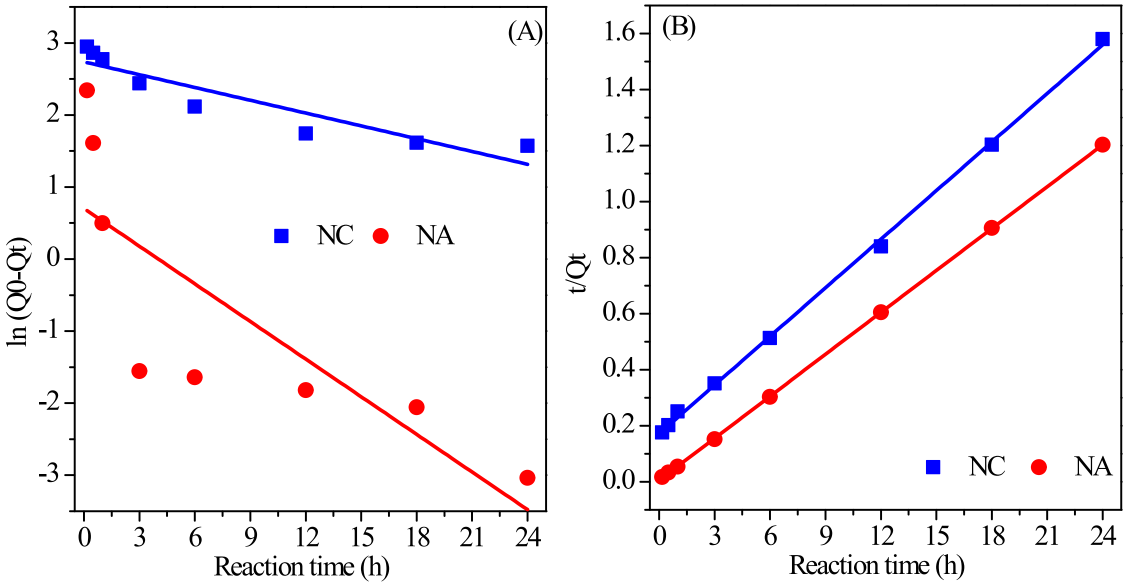

Figure S1. Pseudo-first-order (A) and pseudo-second-order (B) kinetic models of U(VI) on NA and NC, pH 4.0, I = 0.01 mol/L, m/v = 0.5 g/L, T = 293 K.

Table S1. The parameters of pseudo-first-order and pseudo-second-order kinetic model of U(VI) on NA and NC

Adsorbates	Pseudo-first-order			Pseudo-second-order		
	qe (mg/g)	kf (min^{-1})	R^2	qe (mg/g)	ks (g/(mg·min))	R^2
NA	2.017	0.1714	0.6568	20.04	0.4293	1
NC	15.45	0.0593	0.8632	17.31	0.0194	0.9991

Langmuir and Freundlich Equations

Langmuir [5] and Freundlich equations [6] can be described by *Eqns.* (S10) and (S11), respectively:

Langmuir equation:

$$q_e = \frac{q_{max} \times b \times C_e}{1 + b \times C_e}$$

(S10)

Freundlich equation: $$q_e = KC_e^{\frac{1}{n}} \qquad \text{(S11)}$$

where q_e (mg/g) and C_e (mg/L) are the mass of sorbed U(VI) on NA/NC and U(VI) concentration in solution at equilibrium, respectively. b and K are constants of Langmuir and Freundlich model, respectively. $q_{max,}$ (mg/g) are the maximum adsorption capacity at equilibrium.

Table S2 Parameters of Langmuir and Freundlich model for U(VI) adsorption onto NA and NC.

	Adsorption isotherms					
	Langmuir			Freundlich		
	K_a (L/mg)	q_{max} (mg/g)	R^2	$\ln K_F$ ((mg/g)/(mg/L)^n)	$1/n$	R^2
NA	0.1398	188.68	0.9747	3.1033	0.7600	0.9963
NC	1.3790	58.479	0.9994	3.307	0.3548	0.9439

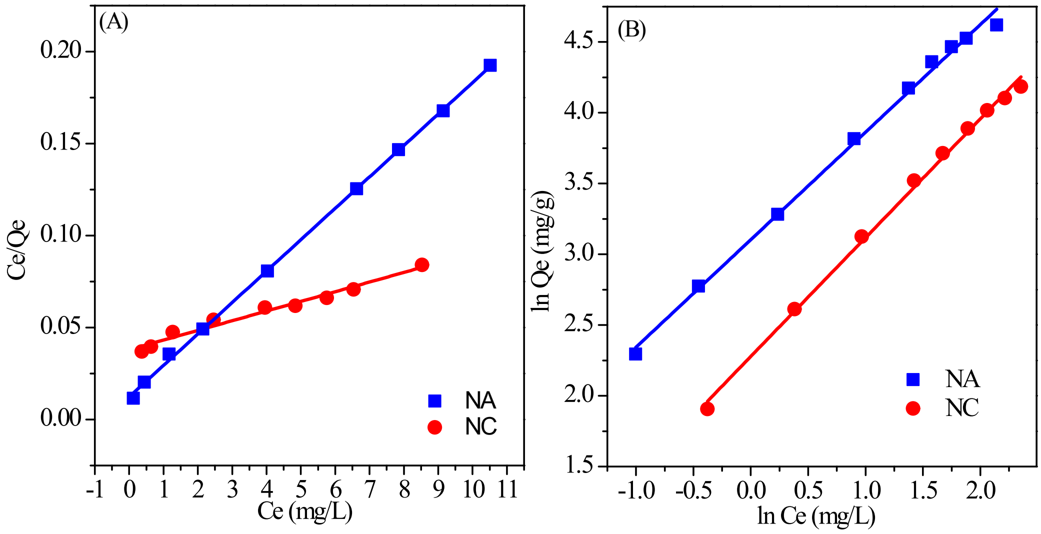

Figure S2. Langmuir (A) and Freundlich (B) kinetic models of U(VI) on NA and NC

Distribution of U(VI) in aqueous solutions

The distribution of U(VI) in aqueous solutions were calculation by visual MINTEQ mode [7]. The distribution of U(VI) speciation in the absence and presence of carbonate was showed in Figure S3A and S3B, respectively.

Table S3 Equilibrium constants for U(VI) species in aqueous solution

Reactions	Log K	Ref.
$UO_2^{2+} + H_2O = UO_2OH^+ + H^+$	-5.20	[8]
$UO_2^{2+} + 2H_2O = UO_2(OH)_2 + 2H^+$	-12.10	[8]
$UO_2^{2+} + 3H_2O = UO_2(OH)_3^- + 3H^+$	-19.20	[8]
$UO_2^{2+} + 4H_2O = UO_2(OH)_4^{2-} + 4H^+$	-33.00	[8]
$3UO_2^{2+} + 5H_2O = (UO_2)_3(OH)_5^+ + 5H^+$	-15.55	[8]
$3UO_2^{2+} + 7H_2O = (UO_2)_3(OH)_7^- + 7H^+$	-28.34	[8]
$UO_2^{2+} + 2CO_3^{2-} = UO_2(CO_3)_2^{2-}$	16.94	[9]
$UO_2^{2+} + 3CO_3^{2-} = UO_2(CO_3)_3^{4-}$	21.60	[9]

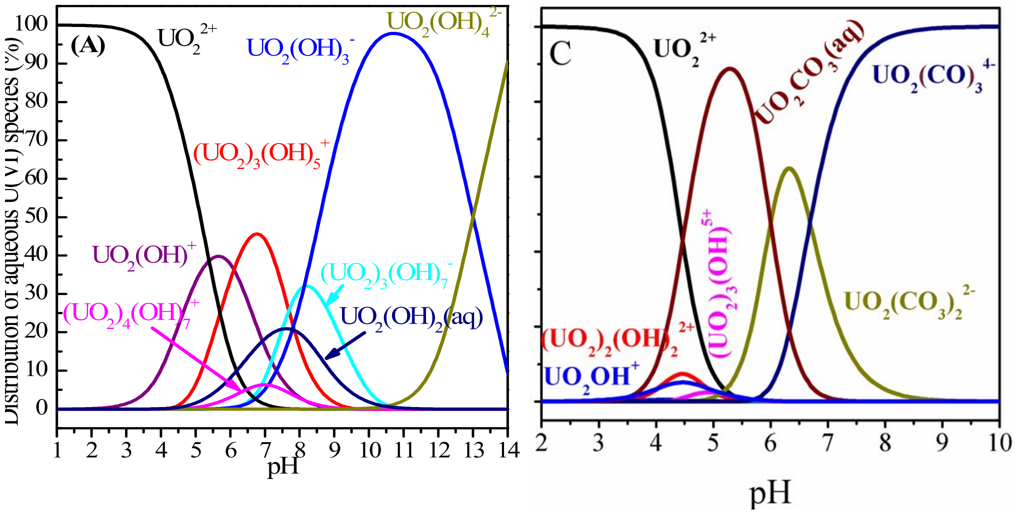

Figure S3. Distribution of U(VI) species in the absence (A) and presence (B) of carbonate, $C_{U(VI)}$ =10 mg/L, $P_{CO_2} = 10^{-3.45}$ atm

Identity of different reactive sites

The weak, strong and very strong sites were determined by extraction of U(VI) from NA/NC using 10 mmol/L Na_2CO_3, 1.0 mol/L Na_2CO_3 and 1.0 mol/L HNO_3 solution, respectively. The values of log Kw, log Ks and log Kss were obtained by fitting desorption data of NA/NC using MINTEQ mode.

Table S4 The percent of different sites for NA and NC

	[U]w	[U]s	[U]ss	Weak site (%)	Strong site (%)	Very strong site(%)
NA	6.17	144.6	4.48	2.26	53.27	1.80
NC	29.55	24.34		26.17	68.05	

References

[1] K.G. Stollenwerk, Modeling the Effects of Variable Groundwater Chemistry on Adsorption of Molybdate, Water Resources Research, 31 (1995) 347-357.

[2] L.S. Balistrieri, J.W. Murray, The Surface-Chemistry of Goethite (Alpha-Feooh) in Major Ion Seawater, American Journal of Science, 281 (1981) 788-806.

[3] S. Lagergren, Zur theorie der sogenannten adsorption geloster stoffe.Pseudo-second order model for sorption processes Handlingar, 24 (1898) 1-39.

[4] Y.S. Ho, G. McKay, Pseudo-second order model for sorption processes, Proc. Biochem., 34 (1999) 451-465.

[5] I. Langmuir, The adsorption of gases on plane surface of glass, mica and platinum, J. Am. Chem. Soc., 40 (1918) 1361-1403.

[6] H.M.F. Freundlich, Uber die adsorption in lasungen, J. Phys. Chem., 57 (1906) 385-470.

[7] J.P. Gustafsson, A windows version of MINTEQ, http://http://www.lwr.kth.se/English/OurSOrware/vminteq/index.htm, (2009).

[8] T.D. Waite, J.A. Davis, T.E. Payne, G.A. Waychunas, N. Xu, Uranium(VI) adsorption to ferrihydrite - application of a surface complexation model, Geochim. Cosmochim. Acta, 58 (1994) 5465-5478.

[9] J.G. Catalano, G.E. Brown, Uranyl adsorption onto montmorillonite: Evaluation of binding sites and carbonate complexation, Geochim. Cosmochim. Acta, 69 (2005) 2995-3005.